Regulation of vitamin D receptor expression by retinoic acid receptor alpha in acute myeloid leukemia cells

Brown, Geoffrey; Marchwicka, Aleksandra ; Cebrat, Magorzata; aszkiewicz, Agnieszka ; nieewski, ukasz ; Marcinkowska, Ewa

DOI:
10.1016/j.jsbmb.2016.03.013

Regulation of vitamin D receptor expression by retinoic acid receptor alpha in acute myeloid leukemia cells.

Aleksandra Marchwicka[1]*, Małgorzata Cebrat[2]*, Agnieszka Łaszkiewicz[2], Łukasz Śnieżewski[2], Geoffrey Brown[3], Ewa Marcinkowska[1#].

*These authors equally contributed to the paper.

[1]Laboratory of Protein Biochemistry, Faculty of Biotechnology, University of Wrocław, Joliot-Curie 14a, 50-383 Wrocław, Poland

[2]Laboratory of Molecular and Cellular Immunology, Department of Tumor Immunology, Institute of Immunology and Experimental Therapy, Polish Academy of Science, Weigla 12, 53-114 Wrocław, Poland

[3]School of Immunity and Infection, College of Medical and Dental Sciences, University of Birmingham, Edgbaston, B15 2TT, UK

[#] Corresponding author: Ewa Marcinkowska, tel. +48 71 375 29 29, ema@cs.uni.wroc.pl

Highlights

- We show that RARα is responsible for regulating *VDR* transcription in AML cells.
- We show that the *VDR* transcriptional 1a variant is regulated by RARα in AML cells.
- *VDR* gene expression is low in the absence of RARα agonist in KG1 cells.
- We identify a *VDR* transcript variant originating from a new exon 1g.
- The *cis*-regulatory element, used by RARα, is located in the promoter region of exon 1a.

Abstract

Acute myeloid leukemia (AML) is the predominant acute leukemia among adults, characterized by an accumulation of malignant immature myeloid precursors. A very promising way to treat AML is differentiation therapy using either all-*trans*-retinoic acid (ATRA) or 1,25-dihydroxyvitamin D_3 (1,25D), or the use of both these differentiation-inducing agents. However, the effect of combination treatment varies in different AML cell lines, and this is due to ATRA either down- or up-regulating transcription of vitamin D receptor (VDR) in the cells examined. The mechanism of transcriptional regulation of *VDR* in response to ATRA has not been fully elucidated. Here, we show that the retinoic acid receptor α (RARα) is responsible for regulating *VDR* transcription in AML cells. We have shown that a *VDR* transcriptional variant, originating in exon 1a, is regulated by RARα agonists in AML cells. Moreover, in cells with a high basal level of RARα protein, the *VDR* gene is transcriptionally repressed as long as RARα agonist is absent. In these cells down-regulation of the level of RARα leads to increased expression of *VDR*. We consider that our findings provide a mechanistic background to explain the different outcomes from treating AML cell lines with a combination of ATRA and 1,25D.

Keywords: vitamin D receptor; retinoic acid receptor alpha; expression; mRNA; target gene; differentiation.

1. Introduction

Acute myeloid leukemia (AML) is the predominant acute leukemia among adults. This disease is difficult to treat due to variable underlying causes and most patients are elderly and often excluded from aggressive chemotherapy trials [1]. A very attractive and gentler way to treat patients with AML is so called differentiation therapy [2, 3]. The most successful differentiation therapy agent is all-*trans*-retinoic acid (ATRA). This is used routinely to treat a very rare form of AML called acute promyelocytic leukemia (APL), in which a PML-RARα fusion protein is generated by a t(15;17)(q22;q12) chromosomal translocation [4]. However, the success of ATRA-based differentiation therapy has not been extended to other forms of AML [5]. 1,25-dihydroxyvitamin D_3 (1,25D) is capable of inducing *in vitro* differentiation of AML cell lines [6], but was not found to be very effective in early clinical trials of AML [7]. Previous work has shown that a combination of 1,25D and ATRA can produce a synergistic differentiation effect [8]. However, our recent research has shown that the effect of this combination treatment varies in AML cell lines [9]. This is due to either down- or up-regulation of vitamin D receptor (VDR) transcription in response to ATRA in the AML cell lines examined. HL60 cells have a high constitutive level of *VDR* mRNA and *VDR* expression is down-regulated by ATRA, whereas KG1 cells have a very low basal level of *VDR* mRNA, and ATRA up-regulates *VDR* expression [9].

The gene encoding human VDR is located on chromosome 12, it covers about 100 kb of genomic DNA [10] and its composition is complex. The gene is composed of 14 exons, and translation of VDR protein spans from the exon 2 to the exon 9 [11, 12]. Due to T to C polymorphism, which eliminates the most 5'-located ATG codon in the exon 2, translation starts from the second in-frame ATG codon in some individuals. Thus, two variants of VDR protein exist, one three amino-acids shorter (aa and 424) than the other (427 aa) [13]. The 5' region is very complex, and consists of the six exons 1a-1f, which together with the corresponding promoter regions are alternatively used in transcription regulation in various tissues [11]. Only three promoter regions have been identified in the region that codes for exons 1a-1f. Transcripts originating from exon 1a and from exon 1d are regulated by the promoter upstream to exon 1a, and exons 1f and 1c have their own upstream promoters (Figure 1A). The regulation of remaining exons remains to be elucidated [11-13].

Transcripts which originate from exon 1a and 1d are expressed in most of the 1,25D-responsive tissues, while a transcript originating in exon 1f is selectively expressed in tissues that play a role in calcium-phosphate homeostasis [11]. Moreover, it has been shown that the transcripts starting from exon 1d give rise to a longer VDR protein, named VDR B1 [11, 14]. ATRA-mediated up-regulation of *VDR* transcription has been reported in the past. However, due to the lack of retinoic acid response elements (RARE) in *VDR* promoter region, the mechanism of the influence of ATRA on

VDR transcription remains unclear. Non-classical ATRA-responsive regions have been reported to be present in a regulatory element localized downstream of exon 1c (as detected in reporter assays using transfected HeLa cells) [13] and in the promoter region upstream of exon 1c (detected in similar assays using breast cancer cells) [15]. It is thus tempting to speculate that the mechanism of regulation of *VDR* by ATRA, and whether the outcome is up- or down-regulation of *VDR* expression, are cell-context dependent.

ATRA is a non-selective agonist of the three distinct isoforms of retinoic acid receptors (RAR) α, β and γ, and these occur as numerous splicing variants [16-18]. RARs, similarly to VDR, form heterodimers with retinoid X receptors (RXR) and act as ligand-regulated transcription factors *via* binding to specific RAREs. However, it should be remembered that un-ligated RARα, and to much lesser extent RARβ and γ, may act as transcriptional repressors to certain genes [19, 20]. Due to the differences in the ligand binding domains of distinct RAR isoforms, it has been possible to synthesize a number of selective RAR agonists and antagonists [21]. The means to selectively activate or inhibit distinct isoforms of RARs have led to discovery of their diverse functions, which often relate to various aspects of cell differentiation [22].

To gain a better understanding of the molecular mechanisms of regulation of *VDR* transcription by RARs in AML cells we have examined the transcriptional variants produced by these cells. We have used a rapid amplification of cDNA ends (5'-RACE) method to investigate this problem. The use of selective RAR agonists has allowed us to identify the isoform of RAR that regulates a transcriptional variant of *VDR* in AML cells. Through luciferase reporter assays, we localized the region in the *VDR* promoter which is involved in the regulation of *VDR* expression in response to ATRA. Finally, we have addressed the role of un-ligated RARα in AML cells by using shRNA gene silencing technology.

2. Materials and Methods

2.1. Cell lines and cultures

HL60 cells were obtained from the local cell bank at the Institute of Immunology and Experimental Therapy in Wrocław, and KG1, U973, MV4-11, MOLM-13 and NB-4 cells were purchased from the German Resource Center for Biological Material (DSMZ GmbH, Braunschweig, Germany). The cells were grown in RPMI-1640 medium with 10% fetal bovine serum (FBS), 100 units/ml penicillin and 100 μg/ml streptomycin (Sigma, St Louis, MO) and maintained at standard cell culture conditions.

2.2. Chemicals and antibodies

1,25D was purchased from Cayman Europe (Tallinn, Estonia) and ATRA was from Sigma. The compounds were dissolved in an absolute ethanol to 1000x final concentrations, and subsequently diluted in the culture medium to the required concentration. AGN191183 (pan RAR agonist), AGN195183 (RARα agonist) and AGN205327 (RARγ agonist) have been described previously [23] and were synthesized at the Shangai Institute of Materia Medica. Tazarotene (RARβγ agonist) [24] and BMS453 (RARβ agonist) [25] were purchased from Tocris Bioscience (Bristol, UK). These compounds were stored at 10 mM concentrations in 50% methanol/50% dimethylsulphoxide at -20°C and subsequently diluted in the culture medium to the required concentration. Rabbit polyclonal anti-RARα (sc-550), anti-actin (sc-1616), anti-Histone H1 (sc-10806) and mouse monoclonal anti-VDR (sc-13133) antibodies were from Santa Cruz Biotechnology Inc. (Santa Cruz, CA). Anti-lamin C2 custom made antibody was a kind gift from Prof. Ryszard Rzepecki (Faculty of Biotechnology; University of Wrocław). Goat anti-rabbit IgG and a goat anti-mouse IgG conjugated to peroxidase were obtained from Jackson ImmunoResearch (West Grove, PA).

2.3. cDNA synthesis and Real-time PCR

Isolation of total RNA, reverse transcription into cDNA and Real-time PCR reactions were performed as published before [9], using CFX Real-time PCR System (Bio-Rad Laboratories Inc., CA). The sequences of *VDR*, *CYP24A1* and *GAPDH* primers and reaction conditions were described previously [26]. The *RARA*, *RARB* and *RARG* primers were obtained from RealTimePrimers.com (Real Time Primers, LLC, PA). The primers for *VDR* variants were: forward for VDR1a: 5'GCGGAACAGCTTGTCCACCC, for VDR1d: 5'GCTCAGAACTGCTGGAGTGG, for VDR1g: 5'TTGCTCATCCAGCTTCCCAGAC, and reverse for all variants was: 5'GAAGTGCTGGCCGCCATTG. Quantification of gene expression was analyzed with either the ΔCq or ΔΔCq method using *GAPDH* as the endogenous control. Primers efficiencies were measured in all cell lines using a Real-time PCR reaction based on the slope of the standard curve. The results were normalized to primer efficiencies to compare gene expression in different cell lines. Real-time PCR assays were performed at least in triplicate.

2.4. Flow cytometry

The expression of cell surface markers of differentiation was determined by flow cytometry. The cells were incubated with 10 nM 1,25D or/and 1 μM ATRA for 96 h, then washed and stained with 1 μl of fluorescently labeled antibodies CD11b/FITC and CD14/PE or with the appropriate

control immunoglobulins (all from ImmunoTools; Friesoythe, Germany) for 1 hour on ice. Next, they were washed with ice-cold PBS and suspended in 0.5 ml PBS supplemented with 0.1% BSA prior to analysis on FACS Calibur flow cytometer (Becton Dickinson, San Jose, CA). The acquisition parameters were set for an isotype control. The experiments were repeated at least three times and data analysis was performed using WinMDI 2.8 software (freeware by Joseph Trotter).

2.5. Identification of transcriptional start sites of VDR transcripts

To identify the transcriptional start sites of *VDR* transcripts, 5'- RACE (rapid amplification of cDNA ends) was used [27]. Ten µg of RNA isolated from unstimulated or ATRA-stimulated HL60 and KG1 cells was digested with calf alkaline phosphatase (CIP, New England Biolabs) in the presence of RiboLock RNase inhibitor for 1 h at 37^{o}C and purified by extraction with TRI reagent. Half of the CIP-digested RNA was treated with tobacco acid pyrophosphatase (TAP, Epicentre) for 1h at 37^{o}C in 10 µl reaction mixture containing TAP buffer, 0.5 U of TAP and 20 U of RiboLock RNase inhibitor. 2 µl of TAP-treated RNA was ligated with a RNA oligonucleotide (5'-GCUGAUGGCGAUGAAUGAACACUGCGUUUGCUGGCUUUGAUGAAA) for 1 h at 37^{o}C in a 10 µl reaction containing 0.3 µg of the oligonucleotide, 5 U of RNA ligase (New England Biolabs), RNA ligase buffer and 20 U of RiboLock RNase inhibitor. Two µl of RNA was then reverse transcribed using SuperScript III reverse transcriptase (Invitrogen) and random hexamers or gene-specific oligonucleotide complementary to exon 2 of *VDR* gene (5'-GCAGCCTTCACAGGTCATAGC). The cDNA was amplified in nested PCR reactions (2 x 20 cycles, annealing temp. 52^{o}C, in the presence of 1.2 M betaine) using primers complementary to 5'-adapter (5'-GCTGATGGCGATGAATGAACACTG, 5'-CGCGGATCCGAACACTGCGTTTGCTGGCTTTGATG) and exon 2 of VDR gene (5'-GCAGCCTTCACAGGTCATAGC, 5'-GTGAAAGCCAGTGGCTCGGT). The amplification products were directly cloned into pGEMT-easy vector. For each type of cell and stimulation 15-20 individual plasmid clones were sequenced using SP6 primer (5'-ATTTAGGTGACACTATAG) and BigDye 3.1 Terminator Cycle Sequencing Kit (Life Technologies). In total, 67 clones were sequenced. The sequencing reaction was analyzed using ABI Prism 310 Genetic Analyzer. The sequences of VDR transcripts obtained were aligned with the genomic sequence of *VDR* gene using Spidey software to identify exons and transcriptional start sites.

2.6. Reporter assays

Two forms of the *VDR 1α* promoter: 1a long (-1935/+71) and 1a short (-464/+71) were cloned upstream of the firefly luciferase gene in the pGL3 Basic vector (Promega) using SLIC cloning. First, promoter fragments were obtained by amplification of the genomic DNA isolated from KG1 cells in a

PCR reaction using Phusion Green High–Fidelity Polymerase (Thermo Scientific) and primer pairs: VDRp1aDF-pGL3, VDRp1aR and VDRp1aKF-pGL3, VDRp1aR-pGL3 for the long and the short form respectively. The SLIC reaction was performed as following: 0.038 pmol of BglII/HindIII-digested pGL3Basic, 0.08 pmol of *VDR 1α* promoter fragment (long or short form), 1 x BSA, 1 x NEB buffer 2, 0.5 µl T4 polymerase were incubated for 2.5 minutes at room temperature in a final volume of 10 µl. Then 20 ng of RecA protein were added and the reaction was stored on ice. Chemically competent DH5α cells were transformed with 5 µl of the reaction product using thermal shock method (45 seconds, 42^{o}C).

For the reporter assays, HL60 cells were co-transfected with 2.5 µg of the reporter pGL3 plasmids and with the 1 µg of the control pRL-TK plasmid, using Neon®Transfection System (Invitrogen™, Carsbad, CA) according to the manufacturer's manual. At 24 h after transfection, the cells were left untreated or stimulated for 96 h with 1 µM ATRA. After that time the luciferase activity was measured with Dual-Glo Luciferase Assay System (Promega Corp., Madison, WI) according to the manufacturer's manual using EnVision Multilabel Plate Reader (Perkin Elmer, Waltham , MS). Firefly luciferase activities were determined in three independent co-transfections and were normalized to the Renilla luciferase activities of the internal control pRL-TK vector from the same culture.

2.7. Gene silencing reagents and procedure

The gene silencing was performed using shRNA lentiviral particles: the *RARA* shRNA lentiviral particles (sc-29465-V) containing three target-specific 19-25nt shRNAs designed to specifically knockdown *RARA* gene expression, and the control shRNA lentiviral particles (sc-108080) containing scrambled shRNA sequences which were used as a negative control (both Santa Cruz Biotechnology, Inc.). KG1 cells were seeded on 24-well plates (2×10^4 cells per well) and after 24 h the cells were infected with 20 µl of lentivirus particles in medium containing 1 µg/ml polybrene (Santa Cruz Biotechnology, Inc.) for 8 h. The medium was changed and the cells were grown for two more days. After that time, the medium was replaced with selection medium containing 1 µg/ml puromycin (Santa Cruz Biotechnology, Inc.).

2.8. Western blots

In order to obtain cytosolic and nuclear extracts $5x10^6$ cells/sample were washed and lysed using Pierce NE-PER Nuclear and Cytoplasmic Extraction Reagents according to the user's manual. Lysates were denatured by adding 5x sample buffer (1/4 volume of the lysate) and boiled for 5 min. 25 µl of each lysate were separated in SDS-PAGE and electroblotted to PVDF membrane. The

membranes were then dried, and incubated sequentially with primary and a horseradish peroxidase-conjugated secondary antibody. The protein bands were visualized by chemiluminescence. Then the membranes were stripped, dried again and probed with subsequent antibodies. Western blots were repeated 3 times.

2.9. Statistical analysis

For statistical analysis one-way ANOVA was used to test the null hypothesis that samples in two or more groups are drawn from populations with the same mean values. When the ANOVA test had shown that the null hypothesis is not true, Student's t-test for independent samples was used to analyze the differences between the pairs of groups (Excel, Microsoft Office and free ANOVA Calculator: http://www.danielsoper.com/statcalc3/calc.aspx?id=43).

3. Results

3.1. Regulation of VDR in response to ATRA in six AML cell lines

Our previous work has shown that transcription of *VDR* gene is regulated in an opposite manner in response to ATRA in two of the commonly used cell lines that typify AML cells. *VDR* transcription was observed to be up-regulated in KG1 cells and down-regulated in HL60 cells. Here, we have examined the regulatory patterns seen in additional human AML cell lines. The molecular and cytogenetic characteristics of the cell lines studied are complex and information is provided in the supplementary Table 1. HL60, KG1, U973, MOLM-13, NB-4 and NOMO-1 cells were exposed for 24, 48, 72 and 96 h to 1 μM ATRA, and the expression of *VDR* was measured by Real-time PCR using *GAPDH* as a reference gene. The highest level of constitutive expression of *VDR* was observed in NB-4 cells (Figure 2A). However, it should be remembered that NB-4 cells harbor one copy of the PML-RARA fusion gene, which encodes the fusion protein PML-RARα. Previous studies have shown that PML/RARα impairs the localization of VDR in the nucleus by binding to VDR and by this means inhibits its transcriptional activity [28]. *VDR* expression was up-regulated by ATRA to a significant extent in NB-4 cells (2.4 times), but to a lesser extent than observed for KG1 cells (more than 7 times). In contrast, *VDR* expression was down-regulated in response to ATRA in HL60 cells (3.2 times), MOLM-13 (2.9 times) and NOMO-1 (5.2 times) cell lines (Figure 2B). The absolute level of *VDR* expression was very low in U937 cells, and it was further down-regulated in response to ATRA (1.8 times). However, this decrease was not statistically significant. Additionally, constitutive *VDR* expression is about 10 times higher in HL60 than in KG1 cells.

The differentiating effects of 1,25D or/and ATRA were examined by flow cytometry. Figures 2C-2H show that for all the cell lines studied the combined effect of ATRA and 1,25D was to increase the level of granulocytic differentiation (increased CD11b expression). The situation was different in regard to expression of monocytic marker CD14. For the cell lines in which ATRA up-regulated *VDR* expression (KG1 and NB-4) combined treatment also up-regulated CD14, when compared to single treatment. For the cell lines in which ATRA down-regulated *VDR* expression it also down-regulated CD14, when compared to 1,25D alone. These results point to increased *VDR* expression shifts the differentiation option from the granulocytic to the monocytic pathway.

3.2. Effects of 1,25D and ATRA on regulation of *CYP24A1* expression

The *CYP24A1* gene encodes the enzyme 24-hydroxylase of 1,25D, which is the key enzyme in the degradation of 1,25D to calcitroic acid. It is well documented that *CYP24A1* is the most strongly regulated of all the 1,25D-target genes [29], thus 1,25D-dependent up-regulation of *CYP24A1* confirms that VDR protein is expressed and active in cells. For the AML cell lines that responded well to 1,25D, the expression of *CYP24A1* was slowly, but significantly, up-regulated up to a thousand-fold, as compared to untreated cells [26]. As shown in Figure 3A and 3C, measurements of *CYP24A1* levels reflected ATRA-driven changes in *VDR* expression and activation levels in KG1 and in HL60 cells. Similarly in MOLM-13 (Figure 3D) and U937 (Figure 3F) cells ATRA-driven changes in *VDR* expression were further reflected in expression of *CYP24A1*. In the case of NB-4 (Figure 3B) and in NOMO-1 cells (Figure 3E) 1,25D-induced *CYP24A1* expression was not altered to a significant degree by ATRA. The data presented in Figure 3 show that ATRA alone does not influence *CYP24A1* expression. Moreover, ATRA-induced changes to *CYP24A1* expression confirmed that increased *VDR* mRNA levels lead to increased translation of VDR protein, which is activated by ligand. It is noteworthy that the observed 1,25D-induced *CYP24A1* expression in HL60 cells is one order of magnitude higher than in MOLM-13 and NOMO-1 cells, two orders of magnitude higher than in NB-4 cells and three to four orders of magnitude higher than in KG1 and U937 cells.

3.3. Transcriptional variants of *VDR* in HL60 and KG1 cells as identified by 5'-RACE

For these studies we chose to use the HL60 and KG1 cell lines as the most sensitive and least sensitive to 1,25D, respectively. We considered that variable regulation of *VDR* gene in these cell lines might result from the usage of different *VDR* promoters. Therefore, we decided to identify the promoter regions that regulate *VDR* transcription in un-stimulated and ATRA-stimulated HL60 and

KG1 cells, and examined the transcript variants occurring in those cells. We used the 5'-RACE method to identify 5' portions of the VDR transcripts - upstream of the *VDR* exon 2. The results of our experiments are presented in Figure 1B and aligned to the published sequence. We found that in both un-stimulated and ATRA-stimulated HL60 cells, *VDR* transcripts originated from exon 1a which was spliced to exon 2 either directly or through exon 1c. The same transcript variants were the most frequently detected transcripts in un-stimulated and ATRA-stimulated KG1 cells. In addition, we observed that KG1 cells express a more diverse set of *VDR* transcripts than HL60 cells. In un-stimulated KG1 cells, we detected transcript variants originating from exon 1d and, from a so-far-unidentified exon, depicted in Figure 1B as exon 1g, and localized downstream of exon 1d. In contrast to HL60, in KG1 cells we detected also exon 1b present in transcripts originating either from exon 1a or 1g. Aside from the differences between HL60 and KG1 cells, the majority of transcripts expressed in both cell types, regardless of the presence or absence of ATRA, originated from exons controlled by the 1a promoter. This strongly suggests a predominant role of the 1a promoter in regulating *VDR* expression in these cells.

3.4. Regulation of *VDR* variants in response to ATRA and to selective RAR agonists

The most frequent transcriptional variants in HL60 and KG1 cells are the ones originating in exon 1a and exon 1d. Hence, we constructed variant-specific primers in order to quantify ATRA-provoked changes in the expression of these transcripts. Our experiments have shown that only the transcript which originates from exon 1a (*VDR 1a*) is regulated in response to 1 μM ATRA. This transcript was significantly down-regulated in HL60 cells (Figure 4A), and significantly up-regulated in KG1 cells (Figure 4B). ATRA is a non-selective agonist of RARα, β and γ. We used selective agonists of RAR isoforms to determine the isoform responsible for regulating the *VDR* transcript that originates from exon 1a. The agents used at a concentration of 100 nM were AGN191183 (pan-RAR agonist), AGN195183 (RARα agonist), tazarotene (RARβγ agonist), AGN205327 (RARγ agonist) and BMS453 (RARβ agonist) and their structures and classification are given in the supplementary Table 2. As shown in Figure 4C (HL60) and 4D (KG1), the pan-RAR agonist, the selective RARα agonist and the mixed RARβγ agonist (tazarotene) significantly regulated transcription of *VDR 1a*. Among the transcript variants of *VDR* gene in KG1 cells we identified rare transcripts, which originated from a newly discovered exon 1g. We tested whether these transcripts are also regulated by the RAR agonists. In HL60 cells such regulation did not occur (not shown), but *VDR1g* transcript appeared to be regulated by RAR agonists in KG1 cells (Figure 4E). The pattern of regulation of *VDR1g* and *VDR1a* in KG1 cells is similar, which suggests that the promoter region used to regulate both transcripts is the same. The data presented in Figure 4 indicate that the most important isoform of RAR involved in

VDR transcription is RARα. Significant up-regulation in KG1 cells, and significant down-regulation in HL60 cells of *VDR1α* by tazarotene suggests that RARβ and γ also have limited regulatory effects, which is further supported by the observation that combination treatment using RARβ and RARγ agonists mimics the effect of tazarotene (not shown here).

3.5. Reporter assays in HL60 cells treated with ATRA

In order to determine whether the promoter of exon 1a responds directly to ATRA stimulation, two reporter vectors were constructed that contained different portions of the 1a promoter regions: -1935/+71 (1a long) and -464/+71 (1a short) relative to the start site of the 1a transcript variant. Transient transfection efficacy was too low in KG1, therefore the activities of the promoter regions could only be tested in HL60 cells. Firefly luciferase activities were normalized to the Renilla luciferase activities of the internal control vector transfected at the same time. The normalized luciferase activities in the cells treated with 1 μM ATRA for 96 h were compared to the respective untreated controls. When Firefly luciferase gene was under the control of 1a short promoter region, no effects of ATRA were observed, but when the 1a long promoter was used luciferase activity was significantly down-regulated by ATRA treatment, in keeping with the regulation of the *VDR 1α* variant in response to ATRA in HL60 cells (Figure 5A).

3.6. Expression of *VDR* in the absence of RARα

Having shown that RARα ligated by its selective agonist regulates transcription of the *VDR* gene in HL60 and KG1 cells, we investigated the role of un-ligated RARα in these cells. Our experiments had shown that constitutive expression of *RARA* mRNA in KG1 cells is much higher than in HL60 cells (Figure 5B). Also the protein level of RARα in the nucleus was higher in KG1 than in HL60 cells (Figure 5C). Even though *RARB* mRNA levels were high in both cell lines, RARβ protein was undetectable in our experiments. *RARG* expression was low in both cell lines, and RARγ protein was not detectable.

Therefore, we silenced the expression of *RARA* in KG1 cells. The gene silencing was performed using *RARA* shRNA lentiviral particles and the scrambled shRNA lentiviral particles as a control. After selecting transduced cells in puromycin containing medium, we obtained two KG1 sublines; KG1-RARα(-), from the use of *RARA* shRNA, and KG1-CTR, from the use of scrambled shRNA. The level of gene silencing was examined by Real-time PCR (Figure 6A) and by Western blotting (Figure 6B, top panel). Whilst RARα silencing was not complete in KG1-RARα(-) cells the level was significant at around 85%. Next, we investigated whether the loss of RARα influenced the basal level

of transcription of *VDR*. The level of *VDR* mRNA in KG1-RARα(-) cells was observed to be almost 5 times higher than in the cells transfected with the control plasmid (Figure 6C). This level was less than the basal level of *VDR* mRNA in HL60 cells, but more than the level in wild-type KG1 cells. In order to confirm that increased expression of *VDR* gene in KG1-RARα(-) cells resulted in the translation of functional VDR protein, we measured VDR protein levels in both sublines. It has been documented earlier that VDR protein is stabilized by 1,25D, and that a high level of VDR in the nucleus can be seen only after addition of 1,25D to AML cells (presented in Figure 5D) [30]. Thus, we exposed KG1-CTR cells and KG1-RARα(-) cells to 10 nM 1,25D for 24 h, or left untreated. As presented in Figure 6D, VDR protein level was observed to be higher in nuclear fractions from KG1-RARα(-) cells as compared to KG1-CTR cells, especially after exposure to 1,25D.

We analyzed the influence of the selective RAR agonists on *VDR* expression levels in both KG1 sublines. KG1-CTR cells were similarly responsive to wild-type KG1 cells, while KG1-RARα(-) had lost responsiveness to RAR agonists. The selective RARα agonist induced a significantly higher *VDR* expression in KG1-CTR cells than any other agonist. The mixed RARβγ agonist (tazarotene) induced significant up-regulation of *VDR*, but to a much lower extent than when the RARα agonist was used alone (Figure 6E).

Discussion

The fact that retinoids regulate the expression of the *VDR* gene in bone and mammary cells is well described, and this effect is known to be cell-type dependent [12, 15]. Also, it is well established that RARα acts as transcriptional repressor when un-ligated [19], and after binding its physiological agonist ATRA then functions to activate transcription [20]. However, precise details are lacking of the molecular events that occur in AML cell lines.

KG1 cells have a high basal level of expression of *RARA* gene, a high constitutive content of RARα protein and a low level of VDR protein. Here, we have shown that un-ligated RARα represses expression of the *VDR* gene in KG1 cells. When KG1 cells were treated with either a selective or non-selective ligand to activate RARα, expression of *VDR* was observed to be up-regulated. A similar effect was obtained by silencing *RARA* gene expression. We interpret these findings to suggest that RARα protein devoid of ligand acts as transcriptional repressor to the *VDR* gene in these cells. Accordingly, HL60 cells have a low constitutive level of expression of *RARA*, a low level of RARα protein, and their basal level of expression of *VDR* is high. Treatment of these cells with a RARα ligand resulted in down-regulation of *VDR* expression, and the reason for this effect remains to be investigated. As to a higher level of RARα in KG1 cells as compared to HL60 cells; KG1 are viewed as

more primitive than the promyeloid cell line HL60 and a change in the level of expression of *RARA* as cells age developmentally may be the underlying reason.

The transcriptional regulation of *VDR* gene is very complex because of the use of several alternative promoter regions in the large regulatory region encompassing 65 kb upstream of the coding region (exons 2–9) [13]. In our studies we have identified transcripts starting from exon 1a within KG1 and HL60 cells. These are the transcripts that are regulated when cells are treated either with ATRA or a RARα specific agonist. From our studies, we have also identified a new non-coding exon, here termed 1g, which either can be used as a transcript start, or alternatively spliced into the transcripts starting from exon 1a.

A more complete understanding of the mechanism whereby expression of the *VDR* gene is regulated in response to retinoids is confounded by the fact that a classical RARE does not exist within the entire *VDR* promoter region. However, it should be remembered that the location of RAREs is highly variable, and ranges from 10,145 bases upstream to 8,141 bases downstream of the 5' end of known transcription start site [31], so the regulatory element does not need to be located in close proximity to the *VDR* gene. It has also been documented that RAREs are often located in intronic regions [32]. Moreover, recent studies have revealed a high level of diversity in the topology and spacing of RAREs. Classical RAREs are composed of two direct repeats of a core hexameric nucleotide sequence, spaced by 1, 2 or 5 random nucleotides (named DR1, DR2 and DR5). New data have revealed that RAREs do not have to be spaced at all (DR0), they can be spaced by 8 nucleotides (DR8) or composed of the inverted repeats (IR) [33]. To circumvent the, as yet, lack of a RARE involved in *VDR* regulation, it has been suggested that retinoids regulate *VDR* transcription in a secondary manner, by using *cis*-regulatory elements which cooperate with the promoter [13]. Until now, these elements have been localized in the vicinity of exon 1c, either downstream [13] or upstream [15], depending on the cell type. Here we have shown for AML cells that a putative *cis*-regulatory element, which is used by RARs, is located in the promoter region of exon 1a, between nucleotides -1935 and -464 relative to the transcriptional start site of 1a. The attempts to specify the exact location of the regulatory element are underway in our laboratories.

As mentioned above, whether ATRA treatment of AML cell lines leads to up- or down-regulation of expression of *VDR* depends on the cell line tested. It is important to bear in mind that several kinase signal transduction pathways are rapidly activated when cells are treated with ATRA. [34]. This, in turn, might influence the phosphorylation status of particular RAR isoforms [35]. Kinase-mediated signaling is also likely to lead to the activation of other transcription factors to change the transcriptional cell landscape. Differences between the AML cell lines as to their signaling and/or transcriptional landscapes may underlie the opposite effects on expression of *VDR* when different

AML cell lines are treated with ATRA. Such considerations are also important to what happens to *VDR* expression when patients' AML cells are treated with ATRA as these cells often have mutations affecting signal transduction pathways. The KG1 cell line alludes to the importance of kinase signaling as these cells harbor a fusion protein kinase FOP2-FGFR1, arising from the FGFR1 Oncogene Partner 2 (FGFR1OP2) - FGFR1 fusion gene, which is constitutively active [36].

The use of 1,25D in combination with ATRA may benefit some but not all AML patients. The addition of ATRA to 1,25D is likely to benefit patients if this leads to up-regulation rather than down-regulation of *VDR*, as in the later case VDR protein is reduced to the detriment of combination differentiation therapy. As shown here, insight to the nature and mechanisms of ATRA-provoked changes to the level of *VDR* expression is important to consideration of the clinical use of ATRA with 1,25D.

Disclosure statement: The authors have no conflict of interest to declare.

Acknowledgements: The research was supported by National Science Centre, Poland (grant No 2015/17/B/NZ4/02632). Publication cost was supported by Wroclaw Center of Biotechnology Program, The Leading National Research Center (KNOW) for years 2014–2018.

References

[1] B. Lowenberg, Acute myeloid leukemia: the challenge of capturing disease variety, Hematology Am Soc Hematol Educ Program, (2008) 1-11.
[2] D. Nowak, D. Stewart, H. Koeffler, Differentiation therapy of leukemia: 3 decades of development, Blood, 113 (2009) 3655-3665.
[3] K. Petrie, A. Zelent, S. Waxman, Differentiation therapy of acute myeloid leukemia: past, present and future, Curr Opin Hematol, 16 (2009) 84-91.
[4] F. Lo-Coco, G. Avvisati, M. Vignetti, C. Thiede, S. Orlando, S. Iacobelli, F. Ferrara, P. Fazi, L. Cicconi, E. Di Bona, G. Specchia, S. Sica, M. Divona, A. Levis, W. Fiedler, E. Cerqui, M. Breccia, G. Fioritoni, H. Salih, M. Cazzola, L. Melillo, A. Carella, C. Brandts, E. Morra, M. von Lilienfeld-Toal, B. Hertenstein, M. Wattad, M. Lübbert, M. Hänel, N. Schmitz, H. Link, M. Kropp, A. Rambaldi, G. La Nasa, M. Luppi, F. Ciceri, O. Finizio, A. Venditti, F. Fabbiano, K. Döhner, M. Sauer, A. Ganser, S. Amadori, F. Mandelli, H. Döhner, G. Ehninger, R. Schlenk, U. Platzbecker, Gruppo Italiano Malattie Ematologiche dell'Adulto; German-Austrian Acute Myeloid Leukemia Study Group; Study Alliance Leukemia, Retinoic acid and arsenic trioxide for acute promyelocytic leukemia, N Engl J Med, 369 (2013) 111-121.
[5] T. Schenk, S. Stengel, A. Zelent, Unlocking the potential of retinoic acid in anticancer therapy, Br J Cancer, 111 (2014) 2039-2045.
[6] E. Abe, C. Miamura, H. Sakagami, M. Takeda, K. Konno, T. Yamazaki, S. Yoshiki, T. Suda, Differentiation of mouse myeloid leukemia cells induced by 1-alpha,25-dihydroxyvitamin D_3, Proc Natl Acad Sci USA, 78 (1981) 4990-4994.
[7] J. Harrison, A. Bershadskiy, Clinical experience using vitamin D and analogs in the treatment of myelodysplasia and acute myeloid leukemia: a review of the literature, Leukemia Research and Treatment [Online], 125814 (2012) 8.

[8] Y. Ma, D. Trump, C. Johnson, Vitamin D in combination cancer treatment, J Cancer, 1 (2010) 101-107.
[9] E. Gocek, A. Marchwicka, H. Baurska, A. Chrobak, E. Marcinkowska, Opposite regulation of vitamin D receptor by ATRA in AML cells susceptible and resistant to vitamin D-induced differentiation, J Steroid Biochem Mol Biol, 132 (2012) 220-226.
[10] A. Baker, D. McDonnell, M. Hughes, T. Crisp, D. Mangelsdorf, M. Haussler, J. Pike, J. Shine, B. O'Malley, Cloning and expression of full-length cDNA encoding human vitamin D receptor, Proc Natl Acad Sci USA, 85 (1988) 3294-3298.
[11] L. Crofts, M. Hancock, N. Morrison, J. Eisman, Multiple promoters direct the tissue-specific expression of novel N-terminal variant human vitamin D receptor gene transcripts, Proc Natl Acad Sci USA, 95 (1998) 10529-10534.
[12] L. Zella, M. Meyer, R. Nerenz, S. Lee, M. Martowicz, J. Pike, Multifunctional enhancers regulate mouse and human vitamin D receptor gene transcription, Mol Endocrinol, 24 (2010) 128-147.
[13] K. Miyamoto, R. Kesterson, H. Yamamoto, Y. Taketani, E. Nishiwaki, S. Tatsumi, Y. Inoue, K. Morita, E. Takeda, J. Pike, Structural organization of the human vitamin D receptor chromosomal gene and its promoter, Mol Endocrinol, 11 (1997) 1165-1179.
[14] K. Sunn, T. Cock, L. Crofts, J. Eisman, E. Gardiner, Novel N-terminal variant of human VDR, Mol Endocrinol, 15 (2001) 1599-1609.
[15] I. Byrne, L. Flanagan, M. Tenniswood, J. Welsh, Identification of a hormone-responsive promoter immediately upstream of exon 1c in the human vitamin D receptor gene, Endocrinology, 141 (2000) 2829-2836.
[16] V. Giguère, E. Ong, P. Segui, R. Evans, Identification of a receptor for the morphogen retinoic acid, Nature, 330 (1987) 624-629.
[17] M. Petkovich, N. Brand, A. Krust, P. Chambon, A human retinoic acid receptor which belongs to the family of nuclear receptors, Nature, 330 (1987) 444-450.
[18] A. di Masi, L. Leboffe, E. De Marinis, F. Pagano, L. Cicconi, C. Rochette-Egly, F. Lo-Coco, P. Ascenzi, C. Nervi, Retinoic acid receptors: From molecular mechanisms to cancer therapy, Mol Aspects Med, 41 (2015) 1-115.
[19] H. Hauksdottir, B. Farboud, M. Privalsky, Retinoic acid receptors beta and gamma do not repress, but instead activate target gene transcription in both the absence and presence of hormone ligand, Mol Endocrinol, 17 (2003) 373-385.
[20] L. Nagy, H. Kao, D. Chakravarti, R. Lin, C. Hassig, D. Ayer, S. Schreiber, R. Evans, Nuclear receptor repression mediated by a complex containing SMRT, mSin3A, and histone deacetylase, Cell, 89 (1997) 373-380.
[21] R. Álvarez, B. Vaz, H. Gronemeyer, Á. de Lera, Functions, therapeutic applications, and synthesis of retinoids and carotenoids, Chem Rev, 114 (2014) 1-125.
[22] H. Wai, Kawakami K, H. Wada, F. Müller, A. Vernallis, G. Brown, W. Johnson, The Development and Growth of Tissues Derived from Cranial Neural Crest and Primitive Mesoderm Is Dependent on the Ligation Status of Retinoic Acid Receptor γ: Evidence That Retinoic Acid Receptor γ Functions to Maintain Stem/Progenitor Cells in the Absence of Retinoic Acid, Stem Cells Dev, 24 (2015) 507-519.
[23] P. Hughes, Y. Zhao, R. Chandraratna, G. Brown, Retinoid-mediated stimulation of steroid sulfatase activity in myeloid leukemic cell lines requires RARalpha and RXR and involves the phosphoinositide 3-kinase and ERK-MAP kinase pathways, J Cell Biochem, 97 (2006) 327-350.
[24] R. Chandraratna, Tazarotene--first of a new generation of receptor-selective retinoids, Br J Dermatol, Suppl 49 (1996) 18-25.
[25] J. Chen, S. Penco, J. Ostrowski, P. Balaguer, M. Pons, J. Starrett, P. Reczek, P. Chambon, H. Gronemeyer, RAR-specific agonist/antagonists which dissociate transactivation and AP1 transrepression inhibit anchorage-independent cell proliferation, EMBO J, 14 (1995) 1187-1197.
[26] H. Baurska, A. Klopot, M. Kielbinski, A. Chrobak, E. Wijas, A. Kutner, E. Marcinkowska, Structure-function analysis of vitamin D_2 analogs as potential inducers of leukemia differentiation and inhibitors of prostate cancer proliferation, J Steroid Biochem Mol Biol, 126 (2011) 46-54.

[27] A. Laszkiewicz, M. Cebrat, A. Miazek, P. Kisielow, Complexity of transcriptional regulation within the Rag locus: identification of a second Nwc promoter region within the Rag2 intron, Immunogenetics, 63 (2011) 183-187.
[28] E. Puccetti, D. Obradovic, T. Beissert, A. Bianchini, B. Washburn, F. Chiaradonna, S. Boehrer, D. Hoelzer, O. Ottmann, P. Pelicci, C. Nervi, M. Ruthardt, AML-associated translocation products block vitamin D_3-induced differentiation by sequestering the vitamin D_3 receptor, Cancer Res, 62 (2002) 7050-7058.
[29] J. Kahlen, C. Carlberg, Identification of a vitamin D receptor homodimer-type response element in the rat calcitriol 24-hydroxylase gene promoter, Biochem Biophys Res Commun, 202 (1994) 1366-1372.
[30] E. Gocek, M. Kielbinski, P. Wylob, A. Kutner, E. Marcinkowska, Side-chain modified vitamin D analogs induce rapid accumulation of VDR in the cell nuclei proportionately to their differentiation-inducing potential, Steroids, 73 (2008) 1359-1366.
[31] J. Balmer, R. Blomhoff, A robust characterization of retinoic acid response elements based on a comparison of sites in three species, J Steroid Biochem Mol Biol, 96 (2005) 347-354.
[32] S. Hua, R. Kittler, K. White, Genomic antagonism between retinoic acid and estrogen signaling in breast cancer, Cell, 137 (2009) 1259-1271.
[33] E. Moutier, T. Ye, M. Choukrallah, S. Urban, J. Osz, A. Chatagnon, L. Delacroix, D. Langer, N. Rochel, D. Moras, G. Benoit, I. Davidson, Retinoic acid receptors recognize the mouse genome through binding elements with diverse spacing and topology, J Biol Chem, 287 (2012) 26328-26341.
[34] M. Giannì, A. Bauer, E. Garattini, P. Chambon, C. Rochette-Egly, Phosphorylation by p38MAPK and recruitment of SUG-1 are required for RA-induced RAR gamma degradation and transactivation, EMBO J, 21 (2002) 3760-3769.
[35] E. Samarut, I. Amal, G. Markov, R. Stote, A. Dejaegere, V. Laudet, C. Rochette-Egly, Evolution of nuclear retinoic acid receptor alpha (RARα) phosphorylation sites. Serine gain provides fine-tuned regulation, Mol Biol Evol, 28 (2011) 2125-2137.
[36] T. Gu, V. Goss, C. Reeves, L. Popova, J. Nardone, J. Macneill, D. Walters, Y. Wang, J. Rush, M. Comb, B. Druker, R. Polakiewicz, Phosphotyrosine profiling identifies the KG-1 cell line as a model for the study of FGFR1 fusions in acute myeloid leukemia, Blood, 108 (2006) 4202-4204.

Figure captions

Figure 1. Organization of the human *VDR locus* and regulation of *VDR* transcription in response to ATRA in AML cells

(**A**) Composition of the 5' regions of *VDR* are according to Crofts et al., 1998 and Zella et al., 2010, and (**B**) shows transcripts identified in our experiments in un-stimulated and ATRA-stimulated HL60 and KG1 cells. For each type of cell and stimulation, 15-20 individual clones were sequenced (67 altogether) and all the variants identified are presented here. Black boxes represent protein coding exons, grey – noncoding exons localized in the regulatory region of the gene. White boxes represent promoter regions. The hatched box represents the newly identified exon (1g). The frequencies of the transcripts identified are given on the left side of their graphical representation.

Figure 2. Regulation of *VDR* transcription and cell differentiation in response to ATRA or/and 1,25D in AML cells

(**A**) Up-regulation of *VDR* expression in response to ATRA in KG1 and NB-4 cells and (**B**) down-regulation of *VDR* expression in response to ATRA in HL60, MOLM-13, NOMO-1 and U937 cells. The cells were exposed to 1 μM ATRA for the times given on the graphs and expression of the *VDR* gene was measured by Real-time PCR relative to *GAPDH* expression levels. The bar charts show mean values (±SEM) of absolute expression levels. Values that differ significantly ($p<0.05$) from those obtained for respective control cells are marked with asterisks.
KG1 (**C**), NB-4 (**D**), HL60 (**E**), MOLM-13 (**F**), NOMO-1 (**G**) and U937 (**H**) cells were exposed to 10 nM 1,25D or/and to 1 μM ATRA for 96 h and CD11b and CD14 differentiation markers were detected using flow cytometry. The bar charts show the mean percentages of CD11b and CD14 positive cells (±SEM). Values that differ significantly ($p<0.05$) from those obtained for 1,25D-treated cells are marked with ¥, while the values that differ significantly ($p<0.05$) from those obtained for ATRA-treated cells are marked by ♦.

Figure 3. Regulation of *CYP24A1* transcription in response to 1,25D or/and ATRA in AML cells

KG1 (**A**), NB-4 (**B**), HL60 (**C**), MOLM-13 (**D**), NOMO-1 (**E**) and U937 (**F**) cells were exposed to 10 nM 1,25D or/and 1 μM ATRA and after 96 h the expression of *CYP24A1* mRNA was measured by Real-time PCR. The bar charts show the mean values (±SEM) of the fold changes in mRNA levels relative to *GAPDH* mRNA levels. Values that differ significantly ($p<0.05$) from those obtained for respective control cells are marked with asterisks, and values that differ significantly ($p<0.05$) in 1,25D+ATRA treated samples *versus* respective 1,25D-treated samples are marked by ¥.

Figure 4. Regulation of *VDR* transcription variants in response to RAR selective and non-selective agonists in HL60 and KG1 cells

Expression and regulation of *VDR 1a* and *VDR 1d* transcriptional variants was examined in HL60 (**A**) and KG1 (**B**) cells by Real-time PCR. The cells were exposed to 10 nM 1,25D or to 1 μM ATRA and

after 96 h the levels of *VDR 1a* and *VDR 1d* mRNA were measured relative to *GAPDH* mRNA levels. Results that differ significantly ($p<0.01$) from respective controls are marked with asterisks.
The influence of non-selective and selective RAR agonists towards *VDR 1a* expression was examined in HL60 (**C**) and in KG1 (**D**) cells. The cells were exposed to 10 nM 1,25D or 100 nM RAR agonists and after 96 h the levels of *VDR 1a* mRNA were measured relative to *GAPDH* mRNA levels by Real-time PCR. The bar charts show the mean values (±SEM) of the fold changes. Results that differ significantly ($p<0.05$) from the respective control are marked with asterisks.
The influence of non-selective and selective RAR agonists towards *VDR 1g* expression was examined in KG1 (**E**) cells. The cells were exposed to 10 nM 1,25D or 100 nM RAR agonists and after 96 h the levels of *VDR 1g* mRNA were measured relative to *GAPDH* mRNA levels by Real-time PCR. The bar charts show the mean values (±SEM) of the fold changes. Results that differ significantly ($p<0.05$) from the respective control are marked with asterisks.

Figure 5. RAR isoforms and VDR in HL60 and KG1 cells

(**A**) Long (-1935/+71) and short (-464/+71) 1a promoter regions were cloned upstream of the Firefly luciferase gene in the pGL3 Basic vector and transfected into HL60 cells together with the control Renilla luciferase vector. The cells were then left untreated or treated with 1 μM ATRA for 96 h and the luciferase activities were measured in these cells. The bar charts show mean values (±SEM) of Firefly/Renilla luciferase units, and the value that differs significantly ($p=0.02$) from the respective control is marked with asterisk.
(**B**) The expression *RARA*, *RARB* and *RARG* was examined in untreated HL60 and KG1 cells by Real-time PCR relative to *GAPDH* expression levels. The bar charts show the mean values of the absolute expression levels (±SEM). Results that differ significantly ($p<0.01$) in KG1 cells from HL60 cells are marked with asterisks.
The levels of RARα (**C**) and VDR (**D**) proteins were determined in the cytosol and nuclei of HL60 and KG1 cells by Western blots. In order to visualize VDR protein, the cells were exposed to 10 nM 1,25D for 24 h. The cytosolic (C) and nuclear (N) extracts were separated by SDS-PAGE, transferred to PVDF membranes and the proteins were revealed using anti-RARα, anti-VDR and anti-actin. The OD ratio of each receptor band was calculated versus the OD of the respective actin band and the means (±SEM) are presented below the blots.

Figure 6. *VDR* in KG1 cells post-silenced expression of RARα

KG1 cells were transformed using lentivirus containing either scrambled shRNA (KG1-CTR) or *RARA* specific shRNA (KG1-RARα(-)). The expression levels of *RARA* mRNA (**A**) and *VDR* mRNA(**C**) in both cell lines were measured by Real-time PCR. The bar charts show the mean values (±SEM) of the fold changes in mRNA levels relative to *GAPDH* mRNA levels. The values that in KG1-RARα(-) cells are significantly ($p<0.01$) different than in KG1-CTR cells are marked by asterisks.
The levels of RARα (**B**) and VDR (**D**) proteins were determined in the cytosol and nuclei of KG1-CTR and KG1-RARα(-) cells by Western blots. In order to visualize VDR protein, the cells were exposed to 10 nM 1,25D for 24 h. The cytosolic (C) and nuclear (N) extracts were separated by SDS-PAGE, transferred to PVDF membranes and the proteins were revealed using anti-RARα, anti-VDR and anti-actin. Anti-Lamin C antibody was used to show the purity of cell fractionation. The OD ratio of each receptor band was calculated versus the OD of a respective actin band and the means (±SEM) are presented below the blots.

(**E**) The expression of *VDR* mRNA was tested by Real-time PCR in KG1-CTR and KG1-RARα(-) cells exposed to 100 nM selective RAR agonists for 96 h. The bar charts show the mean values (±SEM) of the *VDR* mRNA levels relative to *GAPDH* mRNA levels.
The untreated KG1-CTR samples were calculated as 1. The values that differ significantly ($p<0.05$) in treated cells from the respective untreated control are marked by hash. The values that differ significantly ($p<0.05$) from RARα-agonist treated cells are marked by diamond.

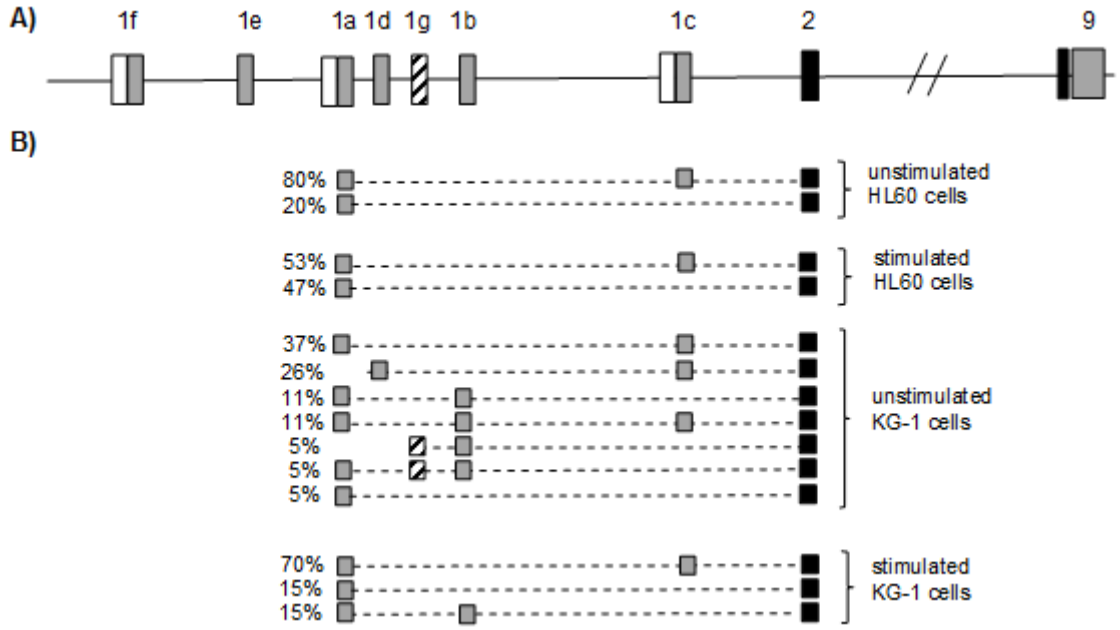
A)
1f
1e
1a
1d
1g
1b
1c
2
9
B)
80%
20%
unstimulated
HL60 cells
53%
47%
stimulated
HL60 cells
37%
26%
11%
11%
5%
5%
5%
unstimulated
KG-1 cells
70%
15%
15%
stimulated
KG-1 cells

Figure 1

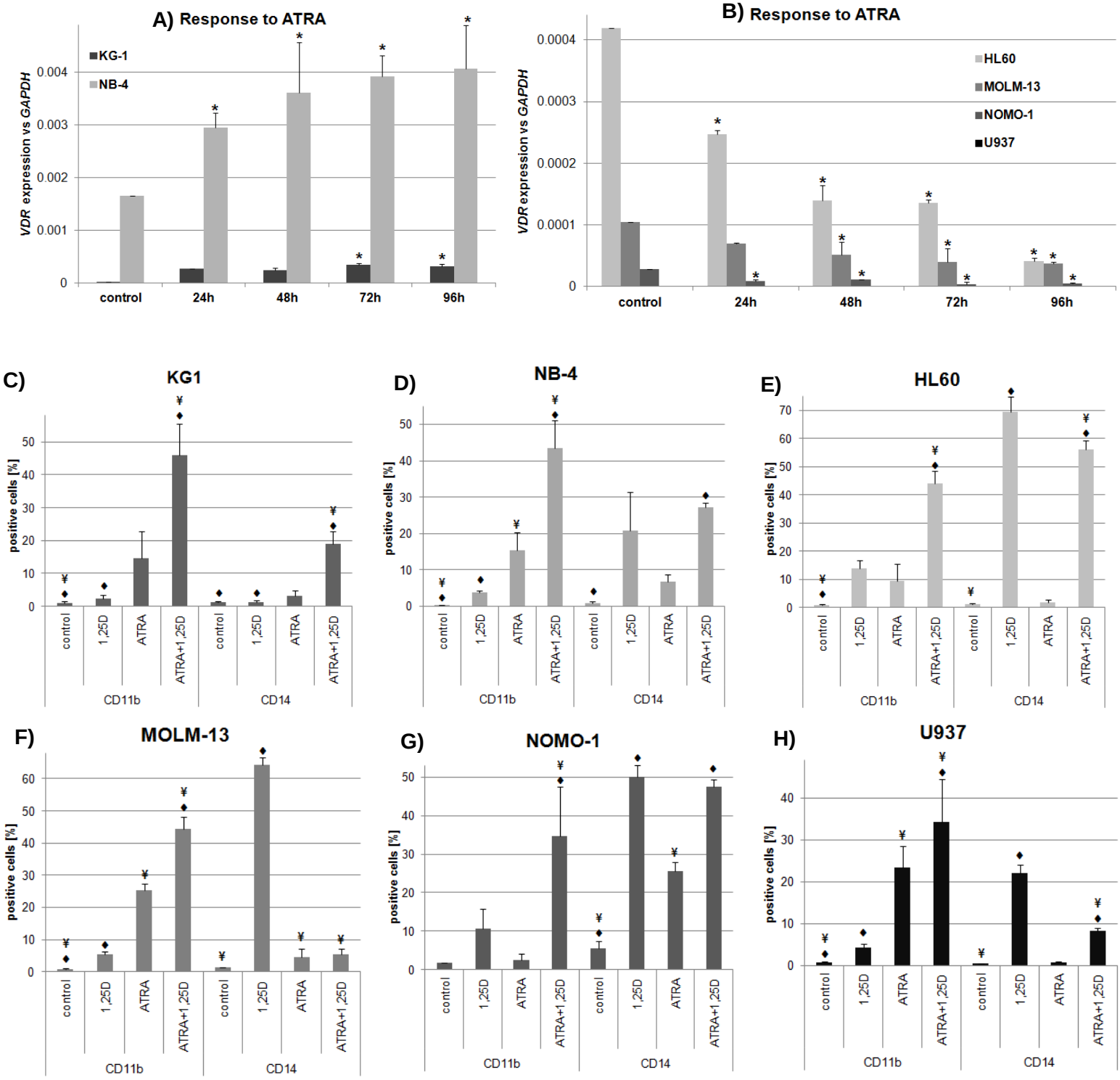
A) Response to ATRA
KG-1
NB-4
VDR expression vs GAPDH
0.004
0.003
0.002
0.001
0
control
24h
48h
72h
96h
B) Response to ATRA
HL60
MOLM-13
NOMO-1
U937
VDR expression vs GAPDH
0.0004
0.0003
0.0002
0.0001
0
control
24h
48h
72h
96h
C)
KG1
D)
NB-4
E)
HL60
F)
MOLM-13
G)
NOMO-1
H)
U937
positive cells [%]
control
1,25D
ATRA
ATRA+1,25D
CD11b
CD14

Figure 2

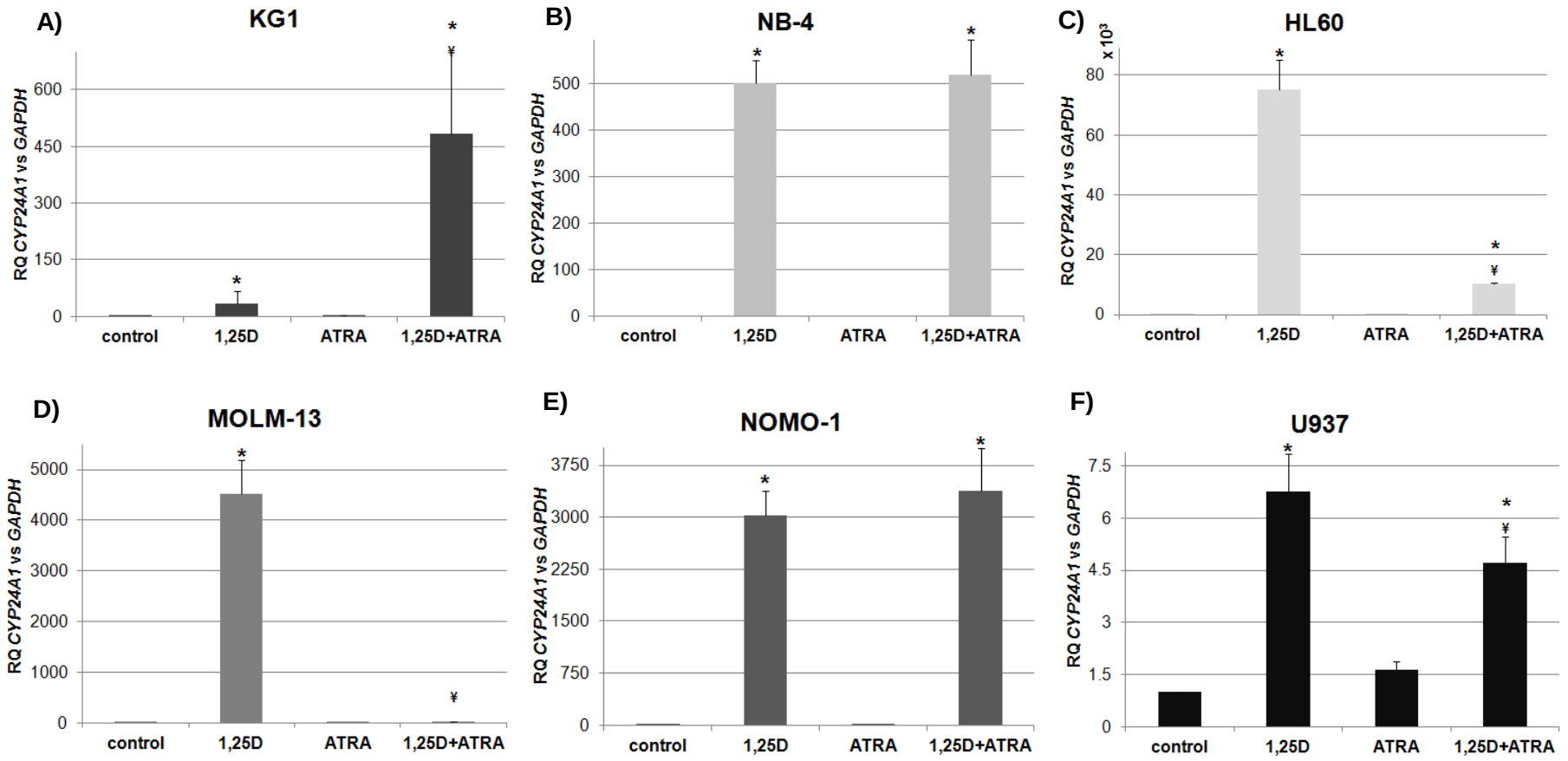
A)
KG1
RQ CYP24A1 vs GAPDH
0
150
300
450
600
control
1,25D
ATRA
1,25D+ATRA
B)
NB-4
RQ CYP24A1 vs GAPDH
0
100
200
300
400
500
control
1,25D
ATRA
1,25D+ATRA
C)
HL60
x 10³
RQ CYP24A1 vs GAPDH
0
20
40
60
80
control
1,25D
ATRA
1,25D+ATRA
D)
MOLM-13
RQ CYP24A1 vs GAPDH
0
1000
2000
3000
4000
5000
control
1,25D
ATRA
1,25D+ATRA
E)
NOMO-1
RQ CYP24A1 vs GAPDH
0
750
1500
2250
3000
3750
control
1,25D
ATRA
1,25D+ATRA
F)
U937
RQ CYP24A1 vs GAPDH
0
1.5
3
4.5
6
7.5
control
1,25D
ATRA
1,25D+ATRA

Figure 3

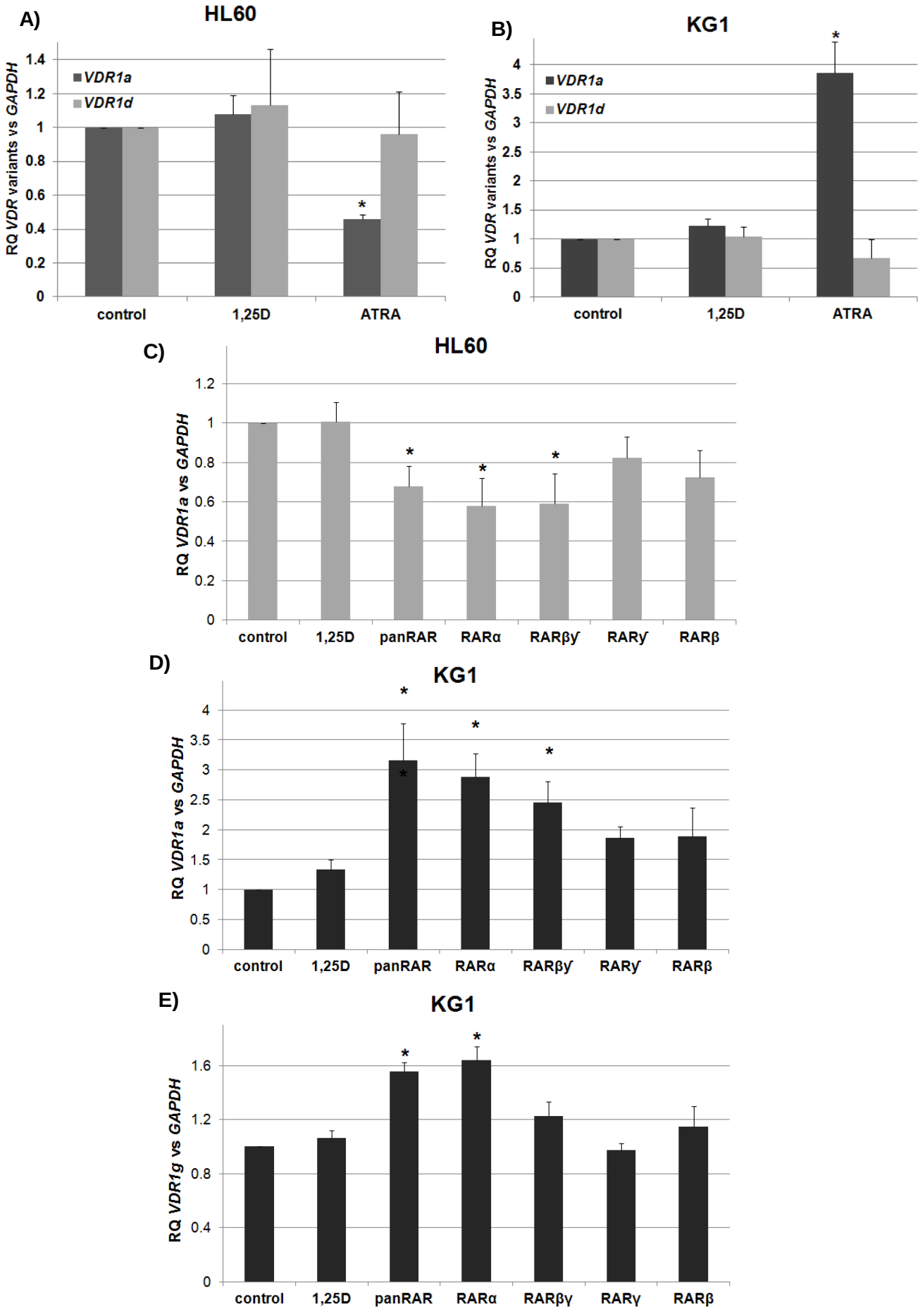
A)
HL60
RQ VDR variants vs GAPDH
VDR1a
VDR1d
control
1,25D
ATRA
B)
KG1
RQ VDR variants vs GAPDH
VDR1a
VDR1d
control
1,25D
ATRA
C)
HL60
RQ VDR1a vs GAPDH
control
1,25D
panRAR
RARα
RARβγ
RARγ
RARβ
D)
KG1
RQ VDR1a vs GAPDH
control
1,25D
panRAR
RARα
RARβγ
RARγ
RARβ
E)
KG1
RQ VDR1g vs GAPDH
control
1,25D
panRAR
RARα
RARβγ
RARγ
RARβ

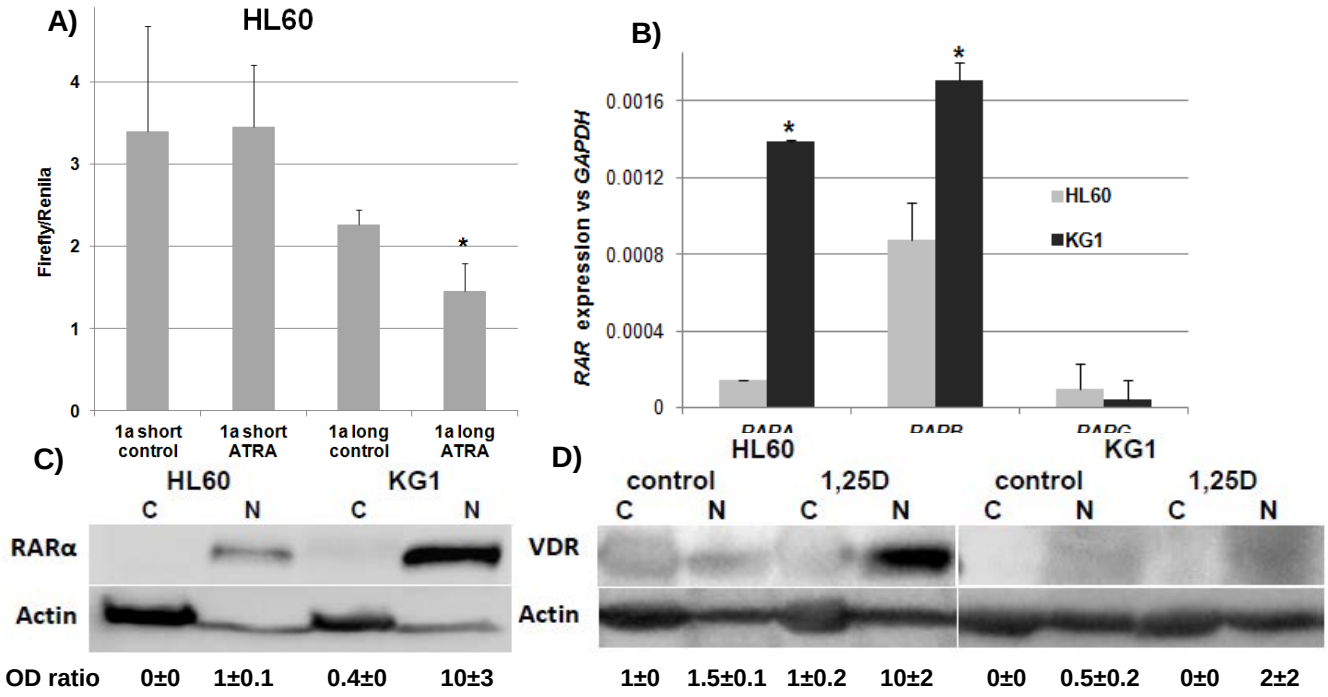
A)
HL60
Firefly/Renilla
0
1
2
3
4
1a short control
1a short ATRA
1a long control
1a long ATRA
B)
RAR expression vs GAPDH
0
0.0004
0.0008
0.0012
0.0016
HL60
KG1
C)
HL60
KG1
C
N
C
N
RARα
Actin
OD ratio
0±0
1±0.1
0.4±0
10±3
D)
HL60
KG1
control
1,25D
control
1,25D
C
N
C
N
C
N
C
N
VDR
Actin
1±0
1.5±0.1
1±0.2
10±2
0±0
0.5±0.2
0±0
2±2

Figure 5

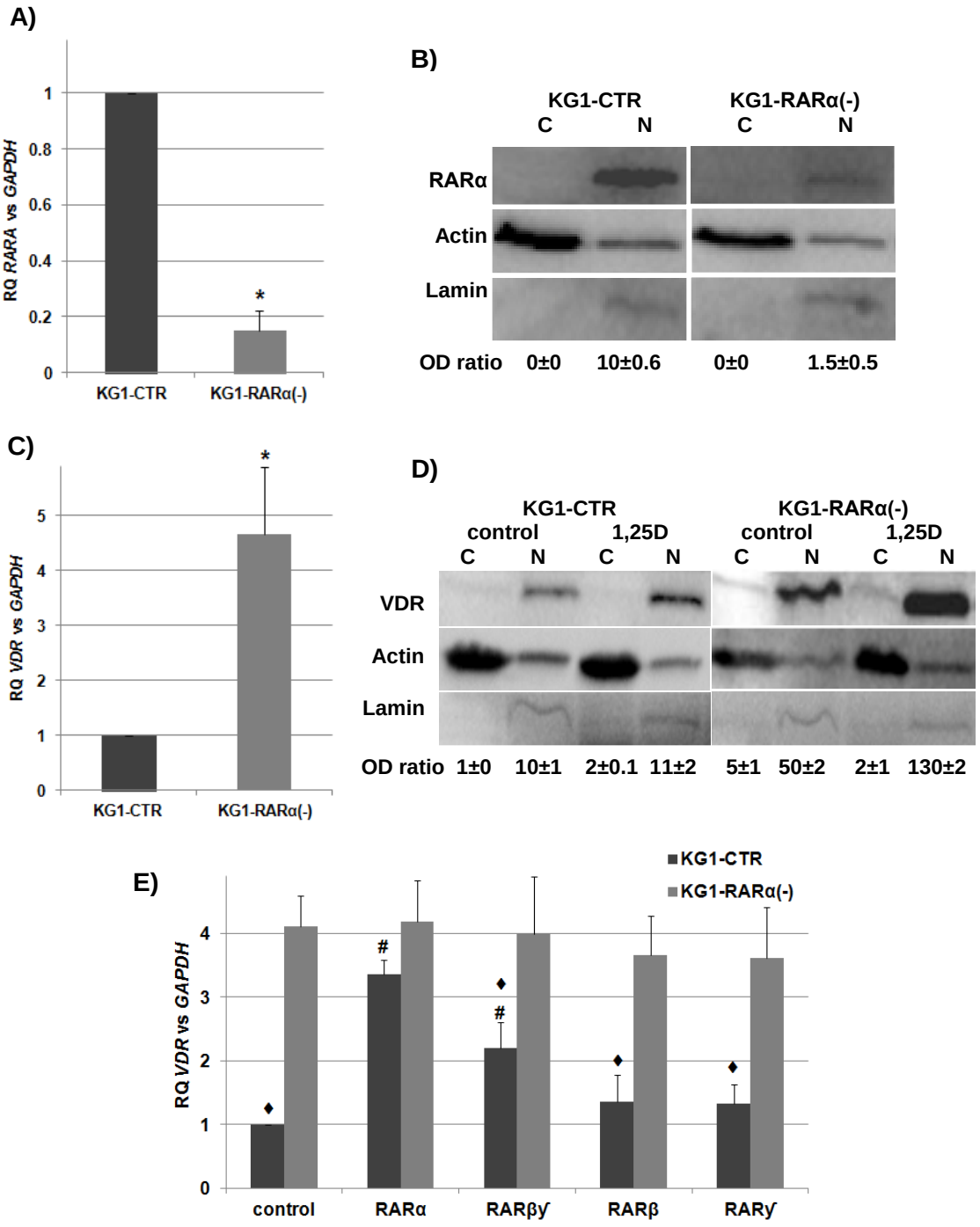
A)
RQ RARA vs GAPDH
1
0.8
0.6
0.4
0.2
0
*
KG1-CTR
KG1-RARα(-)
B)
KG1-CTR
KG1-RARα(-)
C
N
C
N
RARα
Actin
Lamin
OD ratio 0±0 10±0.6 0±0 1.5±0.5
C)
RQ VDR vs GAPDH
5
4
3
2
1
0
*
KG1-CTR
KG1-RARα(-)
D)
KG1-CTR
KG1-RARα(-)
control
1,25D
control
1,25D
C N C N C N C N
VDR
Actin
Lamin
OD ratio 1±0 10±1 2±0.1 11±2 5±1 50±2 2±1 130±2
E)
KG1-CTR
KG1-RARα(-)
RQ VDR vs GAPDH
4
3
2
1
0
#
#
♦
♦
♦
control
RARα
RARβγ
RARβ
RARγ

Figure 6

Supplementary Table 1. Cytogenetic and molecular abnormalities in cell lines studied

	KG-1	HL60	NB-4	MOLM-13	NOMO-1	U937
FAB	AML M5	AML M2	AML M3	AML M5a	AML M5a	
WHO classification	Acute erythroid leukemia	AML with maturation	Acute promyelocytic leukemia (APL)	Acute monocytic leukemia	Acute monocytic leukemia	Histiocytic lymphoma cell line
Karyotype	46,XY,der(4)t(4;8)(q31;p21),−5, del(7)(q22q35), der(8)t(8;12)(p11;q13),+idic(8)(p11)x2,−12, der(17)(5pter⟶5p11::5q13⟶5q31::17p11.2⟶cen⟶17qter),der(20)t(12;20)(?;p13)[20].ish der(4)t(4;8)(*D8Z2*−,*RP11-754L23*−,*MYC*−),der(8)t(8; 12)(*D8Z2*+,*RP11-754L23*+,*MYC*+),+idic(8)(p11)(*D8Z2*++,*RP11-754L23*++,*MYC*++)x2/43∼46, idem,−10[cp4]/46∼47,idem,+der(8)del(8)(p11) del(8)(q11)[cp8]/92∼98,idemx2 [cp2] **[1]**	human flat-moded hypotetraploid karyotype with hypodiploid sideline and 1.5% polyploidy - 82-88<4n>XX, -X, -X, -8, -8, -16, -17, -17, +18, +22, +2mar, ins(1;8)(p?31;q24hsr)x2, der(5)t(5;17)(q11;q11)x2, add(6)(q27)x2, der(9)del(9)(p13)t(9;14)(q?22;q?22)x2, der(14)t(9;14)(q?22;q?22)x2, der(16)t(16;17)(q22;q22)x1-2, add(18)(q21) - sideline with: -2, -5, -15, del(11)(q23.1q23.2) - c-myc amplicons present in der(1) and in both markers **[DSMZ]**	human hypertriploid karyotype with 3% polyploidy - 78(71-81)<3n>XX, -X, +2, +6, +7, +7, +11, +12, +13, +14, +17, -19, +20, +4mar, der(8)t(8;?)(q24;?), der(11)t(11;?)(?->::11p15->11q22.1::11q13->22.1:), der(12)t(12;?)(p11;?), 14p+, t(15;17)(q22;q11-12.1), der(19)t(10;19)(q21.1;p13.3)x2 - identity confirmed	human hyperdiploid karyotype with 4% polyploidy - 51(48-52)<2n>XY, +8, +8, +8, +13, del(8)(p1?p2?), ins(11;9)(q23;p22p23) - resembles published karyotype - sideline with idem, +19 - carries occult insertion effecting MLL-MLLT3 (MLL-AF9) fusion	human hyperdiploid karyotype with 8% polyploidy - 46-47<2n>XX, +8, -13, +mar, add(7)(q32), der(9)del(9)(p11p13-21)t(9;11)(p22;q23), t(9;13)(q13;q11), der(11)t(9;11)(p22;q23) - carries reciprocal t(9;11) with rearrangement of MLL - matches published karyotype	human flat-moded hypotriploid karyotype - 63(58-69)<3n>XXY, -2, -4, -6, +7, -9, -20, -21, +3mar, t(1;12)(q21;p13), der(5)t(1;5)(p22;q35), add(9)(p22), t(10;11)(p14;q23), i(11q), i(12p), add(16)(q22), add(19)(q13) - carries t(10;11) (seen in AML M5) - t(1;5) resembles variant of t(2;5)

			[DSMZ]	**[DSMZ]**	**[DSMZ]**	**[DSMZ]**
Gene fusion	FGFR1OP2-FGFR1 (OP2-FGFR1) **[2]**		PML-RARA (L-form) **[3]**	MLL-MLLT3(MLL AF9) fusion	MLL-MLLT3 (MLL-AF9)	*AF10/CALM* **[4, 5]**
Amplifica-tions	No more than 6 *c-myc* copies **[1]** +8(p11q11)**[6]**	*c-myc* gene **[7, 8]** amp(8)(q24) genes: *MYC, FLJ32440, TRIB1* **[6]**	amp(8)(q24) *FLJ32440, TRIB1, MYC* amp(9)(P24) *JAK2* amp(12)(p12) *KRAS* amp(19)(p13) *TYK2, ICAM1* amp(19)(q13) *CARD8* +2, +10q, +20 **[6]**			*Cyclin D3* **[9]**
Rearranged genes		GM-SCF gene is rearranged and partially deleted (5q21 – 32) **[10]**				
Mutations	TP53 inserted 5 bases (ATCTG) between codons 224 and 225 **[11]**	*N-ras* (codon 61) **[12]** Most of *p53* gene is deleted and retained part is rearranged **[13]** *Smad5* gene is deleted and retained allele is not mutated **[14]** *Max* gene is deleted and retained allele is not	*K-ras* (A18D) **[9]**	*FLT3* mutation (insertion 21bp) **[16]**	*K-ras* (G13D) **[9]** TP53 del1c **[17]**	Heterozygous loss (allele deletion) of *c-Ets-1, T3γ* **[18]** TP53 deleted 46 bases from 1st letter of codon 172 **[11]**

		mutated **[15]**				
Deletions	del(13)**(q14)**, del(16)**(p13p11)**, del(17)**(p13)**, del(1)**(p31p13)**, del(5)**(q21)**, del(7)**(q34q36)**, del(8)**(p22), -12, -17p,** del(18)(q21)	5q11.2-q31, 6q12, 9p21.3-p22, 10p12-p15, 14q22-q31, 16q21, 17p12-p13.3 and –X **[19]**	-1, -3, -5q (*hTERT*), gain(9)(p24p22), del(9)(p21) (*CDKN1B*), gain(13)(q14), del(17)(p13) (*TP53*) **[6, 20]**			

DSMZ Deutsche Sammlung von Mikroorganismen und Zellkulturen GmbH, Braunschweig, Germany

[1] K. Mrózek, S. Tanner, K. Heinonen, C. Bloomfield, Molecular Cytogenetic Characterization of the KG-1 and KG-1a Acute Myeloid Leukemia Cell Lines by Use of Spectral Karyotyping and Fluorescence in Situ Hybridization, Genes, chromosomes & cancer 38 (2003) 249-252.
[2] T. Gu, V. Goss, C. Reeves, L. Popova, J. Nardone, J. Macneill, D. Walters, Y. Wang, J. Rush, M. Comb, B. Druker, R. Polakiewicz, Phosphotyrosine profiling identifies the KG-1 cell line as a model for the study of FGFR1 fusions in acute myeloid leukemia, Blood, 108 (2006) 4202-4204.
[3] Y. Li, J. Andersen, A. Zelent, S. Rao, E. Paietta, M. Tallman, P. Wiernik, R. Gallagher, RAR alpha1/RAR alpha2-PML mRNA Expression in Acute Promyelocytic Leukemia Cells: A Molecular and Laboratory-Clinical Correlative Study, Blood 90 (1997) 306-312.
[4] M. Dreyling, J. Martinez-Climent, M. Zheng, J. Mao, J. Rowley, S. Bohlander, The t(10;11)(p13;q14) in the U937 cell line results in the fusion of the AF10 gene and CALM, encoding a new member of the AP-3 clathrin assembly protein family, Proc Natl Acad Sci U S A, 93 (1996) 4804-4809.
[5] M. Narita, K. Shimizu, Y. Hayashi, T. Taki, M. Taniwaki, F. Hosoda, H. Kobayashi, H. Nakamura, N. Sadamori, H. Ohnishi, F. Bessho, M. Yanagisawa, M. Ohki, Consistent detection of CALM-AF10 chimaeric transcripts in haematological malignancies with t(10;11)(p13;q14) and identification of novel transcripts, Br J Haematol, 105 (1999) 928-937.
[6] F. Rücker, S. Sander, K. Döhner, H. Döhner, J. Pollack, L. Bullinger, Molecular profiling reveals myeloid leukemia cell lines to be faithful model systems characterized by distinct genomic aberrations, Leukemia, 20 (2006) 994-1001.
[7] S. Collins, M. Groudine, Amplification of Endogenous Myc-Related DNA Sequences in a Human Myeloid Leukaemia Cell Line, Nature, 298 (1982) 679-681.
[8] R. Dalla-Favera, F. Wong-Staal, R. Gallo, Onc Gene Amplification in Promyelocytic Leukaemia Cell Line HL-60 and Primary Leukaemic Cells of the Same Patient, Nature, 299 (1982) 61-63.
[9] C. Matteucci, R. La Starza, B. Crescenzi, D. Falzetti, S. Romoli, C. Emiliani, A. Orlacchio, P. Marynen, M. Martelli, C. Mecucci, Interpretation of the complex karyotype and identification of a new 6p amplicon by integrated comparative genomic hybridization and fluorescence in situ hybridization on the U937-I cell line, Cancer Genet Cytogenet, 135 (2002) 28-34.

[10] K. Huebner, M. Isobe, C. Croce, D. Golde, S. Kaufman, J. Gasson, The human gene encoding GM-CSF is at 5q21-q32, the chromosome region deleted in the 5q- anomaly, Science, 230 (1985) 1282-1285.
[11] K. Sugimoto, H. Toyoshima, R. Sakai, K. Miyagawa, K. Hagiwara, F. Ishikawa, F. Takaku, Y. Yazaki, H. Hirai, Frequent mutations in the p53 gene in human myeloid leukemia cell lines, Blood, 79 (1992) 2378-2383.
[12] J. Bos, M. Verlaan-de Vries, A. Jansen, G. Veeneman, J. van Boom, A. van der Eb, Three different mutations in codon 61 of the human N-ras gene detected by synthetic oligonucleotide hybridization, Nucleic Acids Res, 12 (1984) 9155-9163.
[13] D. Wolf, V. Rotter, Major deletions in the gene encoding the p53 tumor antigen cause lack of p53 expression in HL-60 cells, Proc Natl Acad Sci U S A, 82 (1985) 790-794.
[14] J. Zavadil, J. Brezinová, P. Svoboda, Z. Zemanová, K. Michalová, Smad5, a tumor suppressor candidate at 5q31.1, is hemizygously lost and not mutated in the retained allele in human leukemia cell line HL60, Leukemia, 11 (1997) 1187-1192.
[15] K. Ryan, F. al-Mulla, T. Jamieson, G. Birnie, Hemizygosity of the MAX gene locus in HL60 cells, Cancer Genet Cytogenet, 107 (1998) 93-97.
[16] F. Xu, T. Taki, H. Yang, R. Hanada, T. Hongo, H. Ohnishi, M. Kobayashi, F. Bessho, M. Yanagisawa, Y. Hayashi, Tandem duplication of the FLT3 gene is found in acute lymphoblastic leukaemia as well as acute myeloid leukaemia but not in myelodysplastic syndrome or juvenile chronic myelogenous leukaemia in children, Br J Haematol, 105 (1999) 155-162.
[17] S. Forbes, J. Clements, E. Dawson, S. Bamford, T. Webb, A. Dogan, A. Flanagan, J. Teague, R. Wooster, P. Futreal, M. Stratton, COSMIC 2005, Br J Cancer, 94 (2006) 318-322.
[18] J. Shipley, D. Sheer, Deletion of c-ets1 and T3 Gamma Loci from the 11q- Chromosome in the Human Monoblastic Cell Line U937, Leukemia research, 13 (1989) 445-450.
[19] C. Ulger, G. Toruner, M. Alkan, M. Mohammed, S. Damani, J. Kang, A. Galante, H. Aviv, P. Soteropoulos, P. Tolias, M. Schwalb, J. Dermody, Comprehensive genome-wide comparison of DNA and RNA level scan using microarray technology for identification of candidate cancer-related genes in the HL-60 cell line, Cancer Genet Cytogenet, 147 (2003) 28-35.
[20] M. Yaghmaie, H. Mozdarani, K. Alimoghaddam, S. Ghaffari, A. Ghavamzadeh, M. Hajhashemi, Characterization of arsenic-induced cytogenetic alterations in acute promyelocytic leukemia cell line, NB4, Med Oncol, 29 (2012) 1209-1216.

Supplementary Table 2. Characteristics of the RAR agonists used in the study

RAR agonists	Classification	Structure	References
AGN191183	pan-RAR agonist	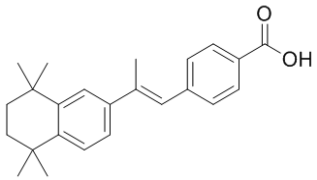	[23]
AGN195183	RARα agonist	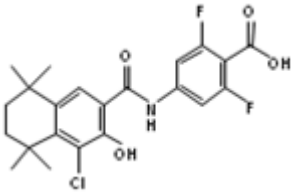	[23]
Tazarotene	RARβγ agonist	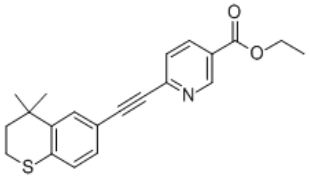	[23, 24]
BMS453	RARβ agonist	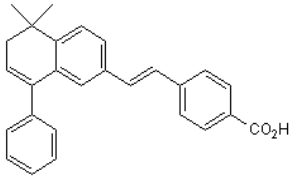	[25]
AGN205327	RARγ agonist	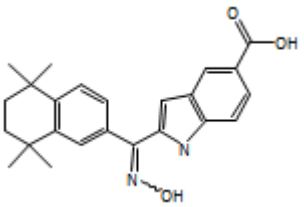	[23]